Development ePress online publication date 12 September 2007

Development 134, 3603-3613 (2007) doi:10.1242/dev.009308

Independent functions and mechanisms for homeobox gene *Barx1* in patterning mouse stomach and spleen

Byeong-Moo Kim[1,2], Isabelle Miletich[3], Junhao Mao[4], Andrew P. McMahon[4], Paul A. Sharpe[3] and Ramesh A. Shivdasani[1,2,5,*]

Homeobox genes convey positional information in embryos and their role in patterning the mammalian gut is a topic of considerable interest. *Barx1* is expressed selectively in fetal stomach mesenchyme and directs differentiation of overlying endoderm. Recombinant tissue cultures and study of young mouse embryos previously suggested that Barx1 controls expression of secreted Wnt antagonists, which suppress endodermal Wnt signaling, to enable stomach epithelial differentiation. We overcame mid-gestational lethality of *Barx1*$^{-/-}$ mouse embryos and report here the spectrum of anomalies in a distinctive and unprecedented model of gastrointestinal homeotic transformation. Using various mouse models, we confirm the importance of attenuated Wnt signaling in stomach development and the role of Barx1 in suppressing endodermal Wnt activity. Absence of Barx1 also results in fully penetrant defects in positioning and expansion of the spleen, an organ that originates within the mesothelial lining of the stomach. Barx1 is absent from the spleen primordium but highly expressed in the mesogastrium, indicating an indirect effect on spleen development. However, our results argue against a role for Wnt antagonism in genesis of the spleen. Mouse spleen development relies on several homeodomain transcriptional regulators that are expressed in the spleen primordium. Loss of Barx1 does not affect expression of any of these genes but notably reduces expression of Wt1, a transcription factor implicated in spleen morphogenesis and expressed in the mesothelium. These observations place Barx1 proximally within a Wt1 pathway of spleen development and reveal how a homeotic regulator employs different molecular mechanisms to mold neighboring organs.

KEY WORDS: Barx1, Mesenchyme-epithelium interactions, Stomach development, Spleen development, Wnt signaling, Organogenesis, Wt1

INTRODUCTION

Lower metazoans meet nutritional needs with a rudimentary intestine that is lined by a simple absorptive epithelium. The more complex nutritional demands in vertebrate animals require additional organs such as the stomach, pancreas and liver, which connect with the small bowel. Early in vertebrate embryogenesis, the visceral endoderm and splanchnic mesoderm combine to create a tube that is subsequently patterned into specialized segments: esophagus, stomach, the intestine and its evaginated derivatives, the liver and pancreas. A component common to all these structures is the mesothelium, a connective tissue that envelops the gut and tethers organs to the body wall. The dorsolateral mesothelium of the stomach (mesogastrium) provides a compartment for early development of the spleen and dorsal pancreas, which appear initially as a confluent primordium near the greater curvature of the stomach (Brendolan et al., 2007; Hecksher-Sorensen et al., 2004; Thiel and Downey, 1921). Stomach rotation and leftward movement of the dorsal pancreas subsequently juxtapose the dorsal and ventral pancreatic buds, which fuse and come to lie near the duodenum, whereas the spleen remains associated with the lateral stomach wall, near its site of origin. Patterning of the rostral gut and its neighboring organs is poorly understood and little is known about the role of mesothelium in their development.

Stomach mesenchymal expression of the homeobox gene *Barx1* seems to be required to suppress regional Wnt activity in prospective gastric endoderm and thus allows stomach-specific epithelial differentiation (Kim et al., 2005). During the period of gastric morphogenesis and gut endoderm specification, *Barx1* is expressed selectively in stomach mesenchyme (Kim et al., 2005; Tissier-Seta et al., 1995). Small-interfering (si) RNA-induced loss of *Barx1* in recombinant cultures of embryonic day (E) 12 mouse fetal tissues profoundly affects differentiation of overlying stomach endoderm: intestinal marker genes are robustly activated at the expense of stomach epithelial transcripts (Kim et al., 2005). *Barx1*-null E12 embryos have normal intestines and a small, aberrantly shaped stomach with atypical endodermal lining; Cdx2, a specific marker of intestinal epithelium (Silberg et al., 2000), is expressed ectopically in the distal stomach. Levels of the secreted frizzled-related proteins Sfrp1 and Sfrp2, soluble antagonists of Wnt signaling (Finch et al., 1997; Rattner et al., 1997), are reduced in the absence of Barx1, and forced Sfrp expression in Barx1-deficient stomach mesoderm restored gastric markers in co-cultured endoderm (Kim et al., 2005).

On the inbred 129/Sv genetic background, *Barx1*$^{-/-}$ mouse embryos die at E13 of unknown causes and so we could not study their subsequent development. Moreover, recombinant fetal tissue cultures convey information about molecular markers but not about histomorphology. Breeding the *Barx1* mutation into a mixed genetic background with contribution from the C57BL/6 strain circumvented embryonic lethality and allowed us to elucidate an unprecedented and completely penetrant patterning defect of the stomach. In addition to this homeotic aberration, Barx1 loss causes a unique defect in development of the spleen, which is consistently mislocalized and severely hypoplastic. As Barx1 is never present in the spleen primordium but highly expressed in surrounding mesogastrium, its effects on spleen development, like those on stomach epithelial specification, must also occur across tissue planes. We confirmed the role of Barx1 in suppressing stomach endodermal Wnt activity, but our studies suggest that its role in

[1]Dana-Farber Cancer Institute and [2]Department of Medicine, Harvard Medical School, Boston, MA 02115, USA. [3]Department of Craniofacial Development, Dental Institute, Kings College, London SE1 9RT, UK. [4]Department of Molecular and Cellular Biology, Harvard University, Cambridge, MA 02138, USA. [5]Department of Medicine, Brigham and Women's Hospital, Boston, MA 02115, USA.

*Author for correspondence (e-mail: ramesh_shivdasani@dfci.harvard.edu)

Accepted 5 August 2007

spleen development is exerted through a different mechanism. In particular, absence of Barx1 specifically reduces mesothelial expression of Wt1, a transcription factor known to be required for spleen morphogenesis. These findings help define the basis for the diverse functions of a homeodomain transcription factor in the development of abdominal organs.

MATERIALS AND METHODS

Experimental animals

Barx1$^{+/-}$ males from the 129/Sv strain were back-crossed repeatedly with heterozygote animals on the C57BL/6 genetic background, and we studied most *Barx1* mutants after at least five back-crosses. TOPGAL transgenic mice and strain-matched CD1 controls were purchased from Jackson Laboratories (Bar Harbor, ME); *Barx1*$^{-/-}$;TOPGAL^{Tg} mice were generated by interbreeding. *Shh*$^{+/Cre}$ mice originated by targeted insertion of a *GFP-Cre* fusion cDNA into the *Shh* locus (Harfe et al., 2004). *Catnb*$^{+/lox(ex3)}$ mice carry an allele with loxP sites flanking exon 3 of the β-catenin (*Catnb*; *Ctnnb1* – Mouse Genome Informatics) gene (Harada et al., 1999) and were generously provided by Mark Taketo (Kyoto University, Japan). *Axin2*^{lacZ} mice have *lacZ* cDNA embedded in the *Axin2* locus (Yu et al., 2005) and were kindly provided by Walter Birchmeier (Max-Delbrück Center, Berlin, Germany). Animals were handled according to protocols approved by an institutional committee. The morning following vaginal plugging was regarded as day 0.5 of gestation.

Histology and immunohistochemistry

After overnight fixation in Bouin's solution or 4% paraformaldehyde, whole embryos or isolated organs were dehydrated, embedded in paraffin and sections of 5-6 μm were prepared. Hematoxylin and Eosin (H&E), PAS and Alcian Blue staining were performed using routine methods. For antigen retrieval prior to immunostaining, specimens were heated in 10 mM Na citrate buffer (pH 6.0) in a decloaking chamber (Biocare Medical, Concord, CA), then cooled for 60 minutes at room temperature. To eliminate endogenous peroxidases, tissues were treated in methanol containing 0.5% H_2O_2 for 30 minutes. After blocking with normal goat serum, samples were incubated for 24 hours at 4°C with one of the following monoclonal antibodies (Ab): Cdx2 (1:20; Biogenex, San Ramon, CA), activated β-catenin (1:500; Upstate Millipore, Charlottesville, VA), Ter119, B220 (Ly76 and Ptprc, respectively – Mouse Genome Informatics) (1:100; B-D Pharmingen, Franklin Lakes, NJ), H^+/K^+-ATPase (2B6, 1:1000; MBL, Nagoya, Japan), smooth muscle actin (1A4, 1:3000; Biogenex) and Muc5ac (45M1, 1:500; Novocastra, Newcastle, UK), or rabbit antisera against gastrin (1:1000; Novocastra), Pdx1 (1:6000; gift of Christopher Wright, Vanderbilt University, TN), insulin (1:1000; Santa Cruz Biotech, Santa Cruz, CA), Barx1 [1:9000 (Kim et al., 2005)], Wt1 (1:3000; Santa Cruz) or Sox2 (1:1000; Chemicon, Temecula, CA). Samples were washed, incubated with biotinylated goat anti-mouse, anti-rabbit or anti-rat IgG and treated with avidin-biotin-peroxidase complex (Vector Laboratories, Burlingame, CA). Color reactions were developed with diaminobenzidine hydrochloride solution (Sigma, St Louis, MO).

β-galactosidase staining

Pregnant dams were sacrificed at various stages and embryos exposed to a β-galactosidase (β-gal) staining protocol that yielded no background in non-transgenic animals (Kim et al., 2005). Briefly, mouse embryos or organs were isolated in Ca^{2+}- and Mg^{2+}-free Hanks' Balanced Salt Solution (Invitrogen, Carlsbad, CA), fixed for 15 minutes with 4% paraformaldehyde in PBS, washed three times in PBS, and incubated in staining solution [PBS (pH 7.2), 1 mg/ml 5-bromo-4-chloro-3-indoyl-β-D-galactoside, 5 mM $K_3Fe(CN)_6$, 5 mM $K_4Fe(CN)_6{\cdot}3H_2O$, 1 mM $MgCl_2$, 0.01% sodium deoxycholate, 0.02 % NP40] for 9-10 hours at 37°C.

In situ hybridization

Sections (6 μm) were cut and mounted on SuperFrost Plus slides (Fisher Scientific, Kalamazoo, MI), deparaffinized, rehydrated, washed in PBS and treated with 1 μg/ml proteinase K (Roche, Indianapolis, IN) for 10 minutes. After acetylation with 0.25% acetic anhydride in 0.1 M triethanolamine (pH 8.0), slides were washed in 2×SSC and air-dried. Hybridization was performed overnight at 60°C with digoxigenin-labeled antisense riboprobes in 50% formamide, 5×SSC, 2×Denhardt's solution, 0.02% bovine serum albumin, 0.1% Tween-20, 0.25% sodium dodecyl sulfate, 5 mM EDTA (pH 8.0) and 50 μg/ml yeast tRNA. Slides were subsequently washed in 2× or 0.2× SSC between 60 and 65°C and again in PBS, followed by incubation for 90 minutes with 20% sheep serum. The hybridized probe was detected by incubating tissue sections overnight at 4°C with alkaline phosphatase-conjugated sheep anti-digoxigenin Ab diluted 1:2000 in PBS supplemented with 5% sheep serum and 5% fetal bovine serum. Color reactions were developed with nitroblue tetrazolium/5-bromo-4-chloro-3-indolyl phosphate (Roche); slides were monitored until color development was observed and the reaction was terminated with distilled water. In situ hybridization with radioactively labeled *Barx1* probe was performed as described previously (Kim et al., 2005).

Transmission electron microscopy

Embryonic stomachs were fixed overnight at 4°C in a solution containing 2.5% paraformaldehyde, 5% glutaraldehyde, 0.06% picric acid, 0.1 M Na cacodylate, and 0.06% $CaCl_2$, post-fixed in OsO_4, and embedded in Epon 812. Thin (0.1 μm) sections were stained with uranyl acetate and lead citrate and examined in a JEOL 1200 electron microscope at an accelerating voltage of 80 kV.

Reverse-transcription (RT)-PCR

Total RNA was extracted using Trizol (Invitrogen), treated with RNase-free DNase (Ambion, Austin, TX) and reverse transcribed using oligo-(dT) primers. *Wt1* mRNA levels were assessed by conventional and SYBR Green real-time quantitative RT-PCR (Applied Biosystems, Foster City, CA) using a common forward primer (5′-GCCTTCACCTTGCACTTCTC-3′) and the reverse primers 5′-CATTCAAGCTGGGAGGTCAT-3′ and 5′-GACCGTGCTGTATCCTTGGT-3′ for conventional and real-time PCR, respectively.

Flow cytometry

Neonatal spleen cells were dislodged with forceps and a single-cell suspension prepared by filtering through a 30-μm strainer. Cells were incubated on ice for 1 hour with 1 μg/ml Ter119, B220, Gr1 (Ly6g – Mouse Genome Informatics), Cd4, Cd8a or Mac1 (Itgam – Mouse Genome Informatics) primary Ab (B-D Pharmingen), followed by washing in PBS and further incubation on ice for 30 minutes with fluorophore-conjugated secondary Ab. Flow cytometry was performed on a Becton Dickinson FACScan and the data were analyzed using FlowJo software (Tree Star, Ashland, OR).

RESULTS

Unique character of gastrointestinal homeosis in the absence of Barx1

We previously implicated the *Barx1*-null mutation in homeotic transformation of the rostral gut; however, unexplained embryonic lethality had restricted analysis to embryos at E12.5 or earlier. Crossing the null mutation [deletion of homeobox-encoding exons 2, 3 and part of exon 4 (Kim et al., 2005)] to introduce the C57BL/6 genetic background permitted *Barx1*$^{-/-}$ mice to survive to birth, although they succumb soon thereafter to respiratory distress that is likely to result from cleft palate; this defect probably reflects significant Barx1 expression in developing branchial arches (see Fig. S1A in the supplementary material) (Tissier-Seta et al., 1995). *Barx1*$^{-/-}$ pups appeared in the expected proportion in over 25 litters and our findings did not vary with C57BL/6 contributions between 50% and 98%. *Barx1*$^{-/-}$ stomach was found to be greatly reduced in size (Fig. 1A) and escaped leftward rotation, thus presenting as a midline structure (data not shown). The villiform lining of neonatal *Barx1*$^{-/-}$ stomach (Fig. 1B) contrasts with the flat mucosa in control mice (Fig. 1D) and carried two distinct surfaces: the distal 1/4 to 1/3 is lined by villi of the intestinal variety, whereas the proximal

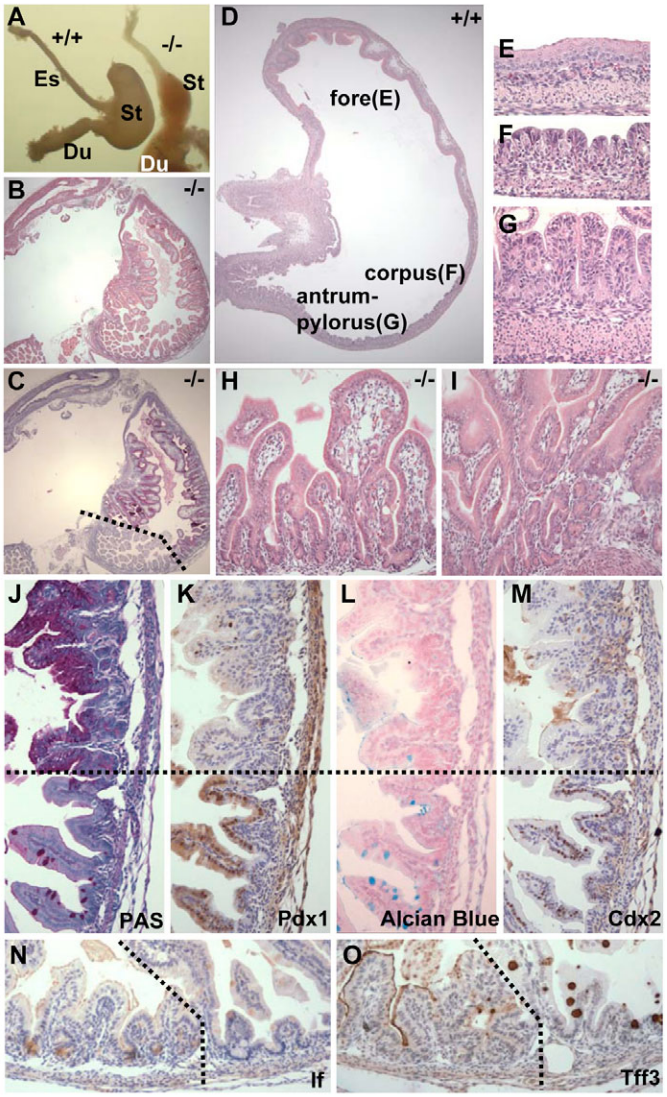

Fig. 1. Gastrointestinal homeosis in the absence of Barx1. (**A**) Comparison of the differences in size and morphology of normal (left) and *Barx1*$^{-/-}$ (right) neonatal stomach, as observed in dozens of embryos and newborn mice. Es, esophagus; St, stomach; Du, duodenum. (**B**,**D**) Mucosal differences between normal (D) and *Barx1*$^{-/-}$ neonatal (B) stomach, revealing a crowded villiform epithelium in the latter. (**C**) Low-magnification micrograph of PAS staining of *Barx1*$^{-/-}$ neonatal stomach, shown to reveal the boundary within the stomach (dotted line) of strongly PAS^{+} gastric mucosa proximally and largely PAS^{-} intestinal epithelium distally. (**E-G**) Normal epithelial histology (H&E stain) from the neonatal mouse forestomach (E), corpus (F) and antrum (G). (**H**,**I**) Gross architectural disorganization typifies the abnormal epithelium (H&E stain) of *Barx1*$^{-/-}$ neonatal mid-stomach. (**J-O**) Histochemical (PAS and Alcian Blue) and molecular [Pdx1, Cdx2, gastric intrinsic factor (If) and trefoil factor 3 (Tff3)] stains highlight the sharp boundary (dotted line) between epithelia of the gastric (top in J-M, left in N,O) and intestinal (bottom in J-M, right in N,O) types in *Barx1*$^{-/-}$ stomach. J-M represent consecutive tissue sections, and N-O are consecutive to each other but not to the others.

stomach has a highly atypical mucosa with gastric features. Periodic acid Schiff (PAS), which stains gastric but not intestinal epithelium uniformly, highlighted this difference (Fig. 1C).

To define the nature of the homeotic transformation, we studied gastric lineage markers. In wild-type mice, a stratified squamous epithelium extends from the esophagus to line the rostral dome (fundus) of the stomach (Fig. 1D,E), followed abruptly by the glandular mucosa of the corpus (Fig. 1D,F), which is flat and carries three major cell types in adults (Karam and Leblond, 1992). In mice, Muc5ac, H^{+}/K^{+}-ATPase and pepsinogen or intrinsic factor (IF; also known as Gif – Mouse Genome Informatics) are specific molecular markers of these respective lineages: foveolar (pit), parietal (oxyntic) and chief (zymogenic) cells. The distal (antral-pyloric) stomach has a similar lining, with modified cell ratios and folds that impart a scalloped appearance (Fig. 1D,G). Neutral mucins in gastric pit cells stain with PAS, whereas intestinal goblet cells are fewer in number and produce acidic mucins with affinity for both PAS and Alcian Blue; intestinal goblet cells also express trefoil factor 3 (Tff3) abundantly (Chinery et al., 1992). Two homeodomain transcription factors permit further distinction between gut segments: Pdx1 expression is scattered in distal stomach and uniform in duodenal epithelium (Offield et al., 1996), whereas Cdx2 is exquisitely specific to the intestine (Silberg et al., 2000). We used these features to characterize *Barx1*$^{-/-}$ stomach.

The mucosal lining of *Barx1*$^{-/-}$ mid-stomach was found to be thickly folded and the glandular morphology highly disorganized, with branching structures and epithelial nests deep in the mesenchyme (Fig. 1H,I). Although this mucosa was folded, it lacked authentic villi and showed characteristic stomach features: apical PAS staining of pit cells, scattered Pdx1 expression and complete absence of Cdx2 or Alcian Blue staining (Fig. 1J-M). By contrast, the intestinal features of the caudal ~1/3 of *Barx1*$^{-/-}$ stomach mucosa were signified by the classic villus morphology, uniform expression of Cdx2 and Pdx1, and presence of goblet cells that stain with Alcian Blue, PAS and Tff3 antibody (Fig. 1J-M,O). A sharp boundary (dotted lines in Fig. 1C,J-O) always separated the intestinal (distal) and gastric (proximal) types of epithelia; cells expressing gastric intrinsic factor (Fig. 1N) and Cdx2 (Fig. 1M) or Tff3 (Fig. 1O), for example, were never mixed. By contrast, although molecular markers of stomach glands were well represented in the proximal mucosa, there was a loss of the usual boundary between corpus and antral epithelia in the *Barx1*$^{-/-}$ mutant. In particular, H^{+}/K^{+}-ATPase- and Pdx1-expressing cells, which normally show little overlap in distribution, mixed freely in the reduced glandular zone in the *Barx1*$^{-/-}$ stomach and Pdx1, normally an antral marker, was expressed in cells abutting the squamous mucosa (Fig. 2A,B).

Proximal *Barx1*$^{-/-}$ foregut showed additional anomalies and even more extensive mixing of cell types. First, radial asymmetry was evident, with a squamous mucosa on one surface and a cuboidal epithelium on the other (Fig. 2C). Second, the differentiated squamous epithelium was interspersed with strongly PAS^{+} cells of the foveolar type (Fig. 2D). These cells, which typify stomach glands and are never seen in normal forestomach or esophagus, appeared throughout the tubular portion of the mutant foregut; we also observed ectopic expression of Muc5ac, the mucin responsible for PAS staining in gastric glands (Fig. 2E). Third, many cells lining the *Barx1*$^{-/-}$ proximal foregut extended numerous apical cilia, a feature restricted to a few scattered cells in control littermates. Ultrastructural analysis highlighted this finding (Fig. 2F), which is characteristic of prospective squamous epithelia and is likely to indicate incomplete differentiation of *Barx1*$^{-/-}$ proximal foregut. Finally, the esophagus was significantly truncated and we never identified a passage lined by a contiguous squamous epithelium; probably as a result of this, the stomach lay mainly in the thorax instead of the abdomen. Thus, judging by its

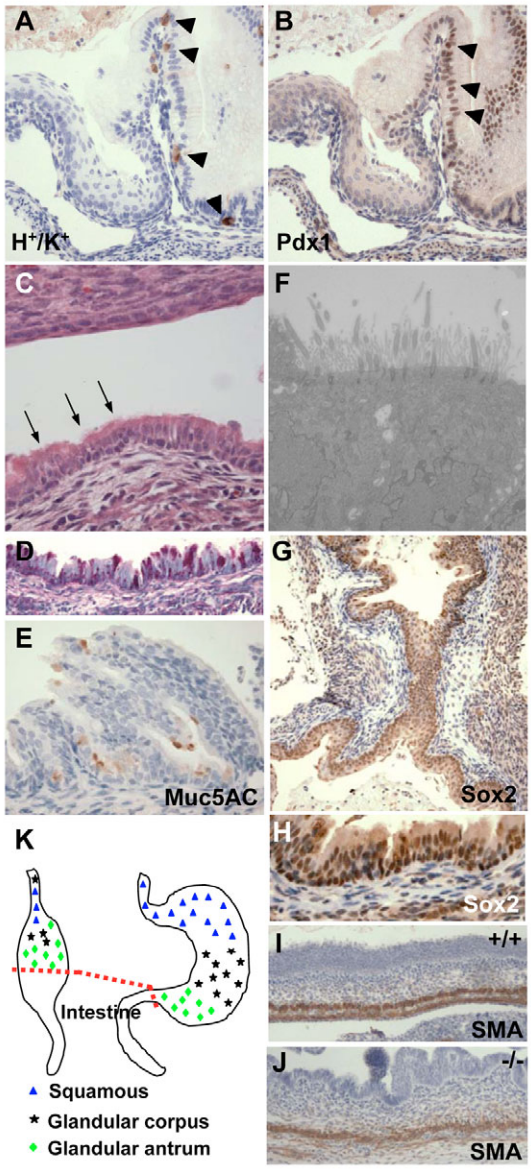

Fig. 2. Severe mucosal abnormalities in the proximal foregut of *Barx1*$^{-/-}$ mice. (**A**,**B**) Abnormally proximal expression of Pdx1 (near the squamous lining) and mixing of H$^+$/K$^+$-ATPase$^+$ and Pdx1$^+$ cells in the glandular mucosa of *Barx1*$^{-/-}$ neonatal stomach. The two panels show staining on adjacent sections. (**C**) Radial asymmetry of the most-proximal mucosa, with one surface lined by a flat squamoid epithelium (seen at the top of the image) and the other (bottom) by a cuboidal epithelium containing many ciliated cells (arrows). (**D**,**E**) PAS (D) and Muc5ac staining (E) reveal the presence in both surfaces of cuboidal cells with features of glandular pit cells. (**F**) Ultastructural confirmation of numerous apical cilia in cells lining neonatal *Barx1*$^{-/-}$ proximal foregut. (**G**,**H**) Immunohistochemical evidence for expression of Sox2, a squamous foregut marker, shown at low (G) and high (H) magnification. (**I**,**J**) Smooth muscle actin staining indicates smooth muscle differentiation in *Barx1*$^{-/-}$ stomach (J), although both signal strength and tissue continuity are reduced in comparison to littermate controls (I). (**K**) Graphic representation of gastrointestinal homeotic and regional anomalies that occur in the absence of Barx1.

epithelium, the structure that overtly resembles an esophagus appeared to be a highly dysmorphic fundus with a mixed squamo-glandular lining. Sox2, a molecular marker of foregut squamous epithelium (Que et al., 2007), was expressed in proximal but not distal *Barx1*$^{-/-}$ foregut (Fig. 2G,H). Cells with smooth-muscle morphology and expression of smooth muscle actin appeared in the correct distribution in the peripheral sub-epithelium, although the muscle layer was discontinuous and less well differentiated than in controls (Fig. 2I,J).

Absence of Barx1 thus results in marked foregut shortening and blurring of gastric squamo-glandular and corpus-antral boundaries (Fig. 2K). We never identified cells with dual stomach-intestine characteristics, but the sharply demarcated gastro-duodenal junction was shifted anteriorly, into the stomach proper. An exterior boundary was always discernible between the stomach and duodenum, but the pyloric sphincter was absent (data not shown). As *Barx1* expression is exclusively sub-epithelial (Kim et al., 2005; Tissier-Seta et al., 1995), the mucosal anomalies in *Barx1*$^{-/-}$ mice must reflect mesenchymal influence over the differentiation of the overlying endoderm. Structural defects such as reduced stomach size, fusiform shape, fundic dysmorphogenesis and pyloric sphincter agenesis, are likely to represent functions intrinsic to the mesenchyme.

Genetic evidence that Barx1 inhibits stomach endodermal Wnt signaling

We previously proposed that Wnt antagonists are prominent targets of Barx1 regulation in gastric mesenchyme (Kim et al., 2005). The prospective stomach shows a wave of Wnt activity after E9, and we proposed that the usual decline in this activity results from Barx1-regulated production of secreted frizzled-related proteins (Sfrps). Recombinant fetal cell culture results supported this idea, but death of *Barx1*$^{-/-}$ embryos precluded direct genetic confirmation. Having overcome fetal lethality, we crossed 129/Sv-C57BL/6 hybrid *Barx1*$^{+/-}$ and TOPGAL transgenic (Tg) mice, which carry *lacZ* cDNA linked to multimerized Wnt-response elements and report faithfully on Wnt signaling (DasGupta and Fuchs, 1999). If the model is correct, proximal stomach endoderm in *Barx1*$^{-/-}$;TOPGAL^{Tg} embryos should, unlike control TOPGAL^{Tg} embryos, continue to express β-gal late in gestation. Indeed, between E16.5 (Fig. 3B) and birth, *Barx1*$^{-/-}$ embryos carrying one copy of the Wnt-reporter transgene showed prominent β-gal activity throughout the proximal foregut, a region we characterized as an atypical gastric fundus with mixed squamous-glandular epithelium (Fig. 2). Residual β-gal activity in control transgenic stomachs was minimal by E16.5 (Fig. 3A,C) and undetectable in E18.5 stomach (data not shown) and at any stage in the developing esophagus. By contrast, the signal in *Barx1*$^{-/-}$;TOPGAL^{Tg} fundic stomach appeared sooner and stronger than in any other site of embryonic Wnt activity; this signal localized to the endoderm (Fig. 3D). We confirmed *lacZ* expression by RNA in situ hybridization in E16.5 foregut, where signal was readily detected in mutant (Fig. 3F) but not control TOPGAL^{Tg} (Fig. 3E) samples.

To monitor Wnt signaling independent of the TOPGAL reporter, we examined β-catenin localization. In E18.5 *Barx1*$^{-/-}$ foregut, innumerable cells showed unambiguous localization in the nucleus (Fig. 3G,H), whereas the signal in littermate control foregut always appeared at cell-cell junctions (Fig. 3I). We also mated *Barx1*$^{+/-}$ mice with another Wnt-reporter strain, *Axin2*^{lacZ}. Insertion of *lacZ* cDNA into the mouse *Axin2* locus, a ubiquitous target of canonical Wnt signaling (Jho et al., 2002), accurately marks sites of Wnt activity (Yu et al., 2005). Again, we readily detected prominent β-gal activity in the atypical fundus in E18.5 *Barx1*$^{-/-}$;*Axin2*^{lacZ} embryos (Fig. 3K), but only weak residual signal in the stomach and none in the esophagus of *Barx1*$^{+/-}$;*Axin2*^{lacZ} littermates (Fig. 3J).

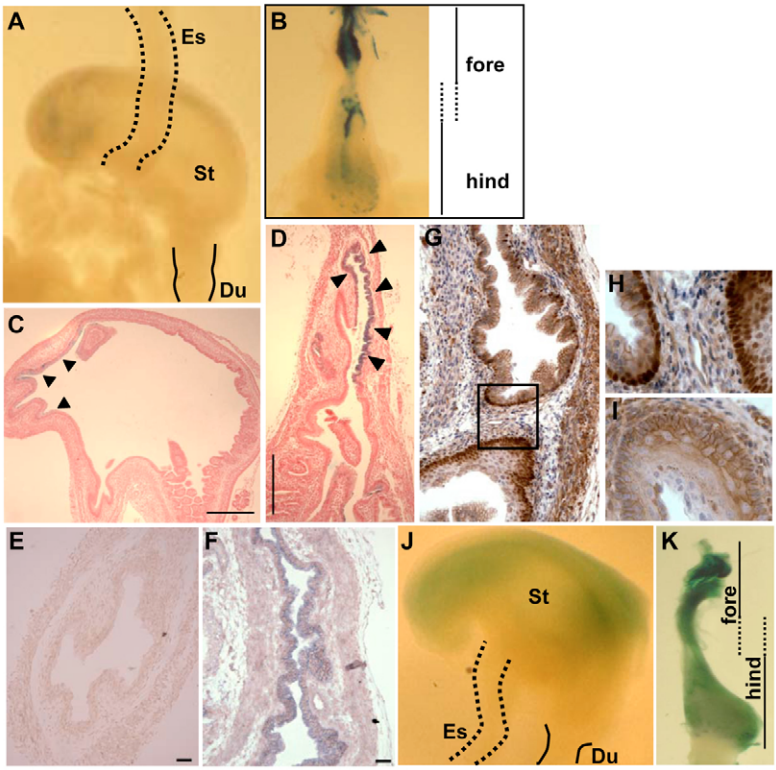

Fig. 3. In vivo confirmation that Barx1 enables attenuation of Wnt signaling in prospective stomach epithelium. (**A**,**B**) *lacZ* staining in *Barx1*$^{-/-}$;TOPGAL^{Tg} (B) and control *Barx1*$^{+/-}$;TOPGAL^{Tg} (A) mouse fetal stomach at E16.5, when endogenous Wnt signaling is virtually abolished and there is no esophageal activity (dashed lines) in control embryos but strong signals remain in *Barx1* mutants. (**C**,**D**) Histochemical confirmation of persistent β-gal activity in rostral *Barx1*$^{-/-}$;TOPGAL^{Tg} stomach endoderm (D, arrowheads) in relation to negligible signal in corresponding *Barx1*$^{+/-}$;TOPGAL^{Tg} tissue (C). (**E**,**F**) Further confirmation by *lacZ* in situ hybridization of mRNA persistence in rostral E16.5 *Barx1*$^{-/-}$;TOPGAL stomach endoderm (F), which contrasts with the absence of expression in control E16.5 *Barx1*$^{+/+}$;TOPGAL tissue (E). (**G-I**) Persistent Wnt signaling is further revealed by nuclear localization of β-catenin in the emerging squamous epithelium of *Barx1*$^{-/-}$ (G, boxed area shown at higher magnification in H) but not control (I) foregut. (**J**,**K**) Similarly, β-gal activity persists in E18.5 *Barx1*$^{-/-}$;*Axin2*^{lacZ} fetal stomach (K) compared with *Barx1*$^{+/-}$;*Axin2*^{lacZ} controls (J). Dashed and solid lines in A and J demarcate normal esophagus (Es) and duodenum (Du), respectively. St, stomach; fore, forestomach; hind, hind-stomach (the blurred boundaries between fore- and hindstomach are represented by dotted lines). Scale bars: 75 μm in C; 60 μm in D; 75 μm in E,F.

Together, these data powerfully validate the idea that Barx1 functions in part to attenuate Wnt signaling in developing stomach endoderm.

To test the model independent of Barx1, we evaluated the consequences of forced β-catenin activation, an obligate mediator of canonical Wnt signaling (Clevers, 2006). We crossed mice carrying a floxed, activating β-catenin allele (Harada et al., 1999) with those expressing Cre recombinase under control of the endogenous sonic hedgehog (*Shh*) gene (Harfe et al., 2004). As *Shh* is highly expressed in stomach endoderm by E8.5 (Echelard et al., 1993), the progeny from this mating should express unrestrained Wnt activity in epithelial progenitors. Crosses between *Shh*$^{Cre/+}$ and ROSA26R mice (Soriano, 1999) indicated efficient Cre-mediated recombination in E10.5 embryos (data not shown) and we detected significant nuclear β-catenin in E18.5 *Shh*$^{Cre/+}$;*Catnb*$^{+/lox(ex3)}$ foregut mucosa (Fig. 4A,B). This experimental model mimics local Wnt activation, although differences in timing and dose might not replicate the *Barx1*$^{-/-}$ stomach exactly. Nevertheless, stomach size was reduced in *Shh*$^{Cre/+}$;*Catnb*$^{+/lox(ex3)}$ embryos and its glandular epithelium resembled that of the *Barx1*$^{-/-}$ gastric corpus (Fig. 1B,H,I): it was thickly folded, branched and contained many epithelial nests deep in the mesenchyme (Fig. 4C,E). As in *Barx1*$^{-/-}$ fundus (Fig. 2C,D), the lining of the distal esophagus was radially asymmetric, with well-formed squamous mucosa on one side and cuboidal epithelium containing PAS-staining cells on the other (Fig. 4F,G). Although intestinal villi were absent from *Shh*$^{Cre/+}$;*Catnb*$^{+/lox(ex3)}$ stomach, the abnormal gastric epithelium contained many cells expressing Cdx2 (Fig. 4H,I), an intestinal epithelial marker (Silberg et al., 2000) that is never found in normal stomach epithelium (Fig. 4J and data not shown). Ectopic β-catenin activation in the developing mouse stomach therefore mimics the heterotopia seen in *Barx1*-null embryos, albeit with some differences, and confirms that attenuation of endogenous Wnt activity is required for normal stomach epithelial differentiation.

Unexpected and unusual requirement for Barx1 in spleen development

The position, size, morphology and histology of lower abdominal organs are preserved in *Barx1*$^{-/-}$ embryos and neonates (data not shown). By contrast, the spleen never appeared in the usual position, apposed to the greater curvature of the stomach, as shown in Fig. 5A for a control neonate; instead, it was markedly hypoplastic and embedded within the dorsal pancreas (Fig. 5B). Associated with this fully penetrant anomaly was failure of the dorsal and ventral pancreatic buds to fuse (Fig. 5B), a defect we attribute to the absence of stomach rotation. *Barx1*$^{-/-}$ spleen harbored typical blood cells, including those with the size and features of megakaryocytes (Fig. 5C and data not shown), and insulin (Fig. 5D) and Pdx1 (red box in Fig. 7D) immunostaining confirmed that they reside in the immediate vicinity of the pancreas. Flow cytometric and immunohistochemical analyses revealed normal proportions of all blood lineages (Fig. 5E and data not shown). Thus, Barx1 loss mispositions the spleen and causes marked hypoplasia without compromising blood or lymphocyte colonization per se.

As in control littermates (Fig. 6A), the pre-splenic mesenchyme appeared in E9.5 *Barx1*$^{-/-}$ mouse embryos as a cell aggregate within the dorsal mesogastrium, next to the dorsal pancreatic anlage (Fig. 6B). Focal β-gal activity in E10.5 and E11.5 *Barx1*$^{-/-}$ embryos that also carry the *Tlx1*^{lacZ} knock-in reporter gene (Kanzler and Dear, 2001) confirmed activation of a genetic program for spleen specification (data not shown; Tlx1 is also known as Hox11). Whereas mesothelial invagination normally separates the spleen and dorsal pancreas as they enlarge in the ensuing 2 days (Fig. 6C), *Barx1*$^{-/-}$ spleen showed little growth and remained attached to the pancreatic primordium (Fig. 6D). To understand the basis for the unexpected role of Barx1 in spleen development, we re-examined its expression domain. At E9.5 and E10.5, Barx1 expression is reported in a columnar cell layer termed the splanchnic mesodermal plate, which is likely to correspond to the future spleen capsule

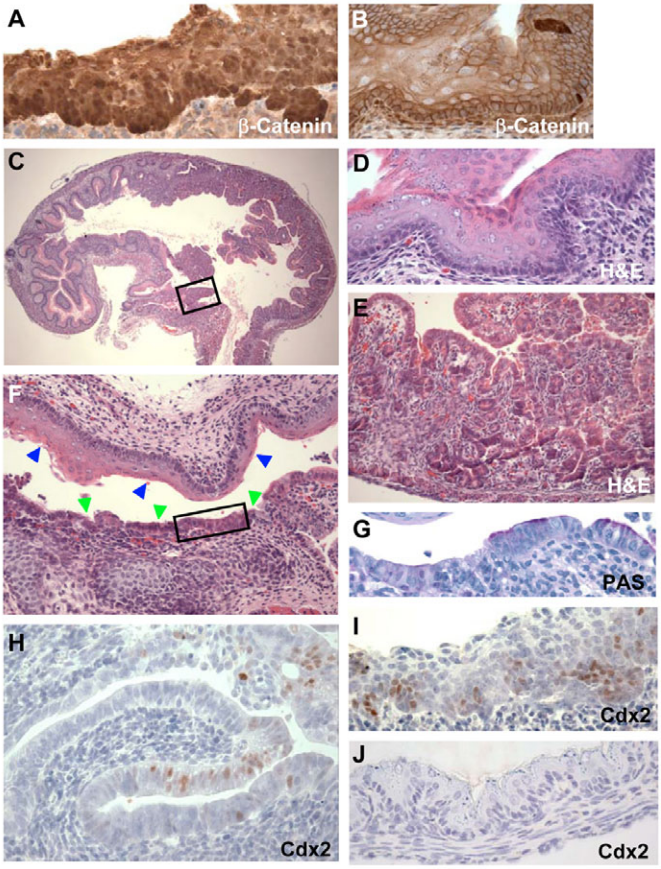

Fig. 4. Independent confirmation of the adverse effects of unregulated Wnt signaling in developing stomach endoderm. Findings in E18.5 $Shh^{Cre/+};Catnb^{+/lox(ex3)}$ mouse embryos. (**A**,**B**) Constitutive β-catenin activation is confirmed by its nuclear staining (A), compared with membrane staining in areas that escaped Cre-mediated recombination (B). (**C-E**) The stomach is reduced in size and lined by a crowded, villiform epithelium (C,E; H&E stain) that shares features seen in *Barx1* mutant stomach, including thick folds and mucosal invasion of the mesenchymal layer (E), which contrasts with relatively normal squamous differentiation (D) in many areas. (**F**) Radial asymmetry of E18.5 $Shh^{Cre/+};Catnb^{+/lox(ex3)}$ esophagus, with squamous (blue arrowheads) and cuboidal (green arrowheads) epithelia on opposite surfaces. (**G**) Magnification of the area boxed in F. PAS staining reveals many cells abnormally producing mucin in the cuboidal epithelium of the esophagus. (**H-J**) Although intestinal villi are absent, there is considerable and ectopic expression of the intestinal marker Cdx2 (H,I), which is normally excluded from the squamous (J) and glandular (data not shown) stomach. H is a magnification of the area boxed in C.

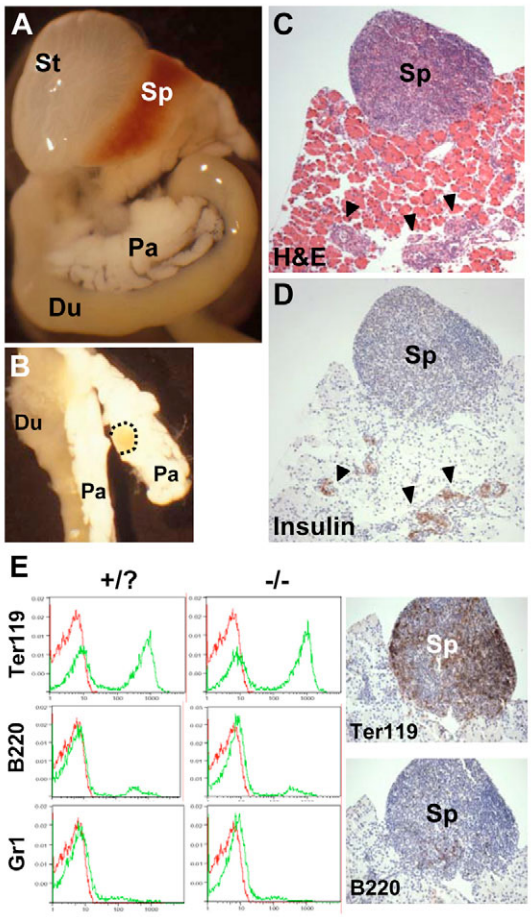

Fig. 5. Abnormal spleen development in *Barx1*$^{-/-}$ mice. (**A**) Relationship of the spleen (Sp) in normal neonatal mice to adjacent stomach (St), duodenum (Du) and a fused pancreas (Pa). (**B**) Invariant size and location of the *Barx1*$^{-/-}$ spleen as a small tissue (marked with a dotted line) attached to the dorsal pancreas, which is separate from the ventral pancreatic bud. (**C**,**D**) Histologic elucidation of intimate association between splenic and pancreatic parenchyma by H&E stain (C) and insulin immunostaining of prospective pancreatic islets (D, arrowheads) on consecutive tissue sections. (**E**) Flow cytometric (left) and immunohistochemical (right) analysis of control (+/?) and *Barx1*$^{-/-}$ spleen (Sp), indicating normal hematopoiesis and lymphoid colonization (+/? refers to +/+ or +/–). Ter119, B220 and Gr1 are specific markers of red cells, B lymphocytes and granulocytes, respectively. Control and *Barx1*$^{-/-}$ spleen also showed identical flow cytometry profiles for T-cell and monocyte surface markers (data not shown).

(Hecksher-Sorensen et al., 2004). We observed that the level of *Barx1* mRNA in this structure, which is contiguous with the mesogastrium, was comparable to that in stomach mesenchyme, but *Barx1* mRNA was excluded from wild-type spleen anlage at all stages, including and beyond E9.5 (Fig. 6E-G and see Fig. S1A in the supplementary material). A specific antiserum helped verify prominent mesothelial expression of Barx1 protein (Fig. 6J,K). Both mRNA and protein staining indicated that mesothelial Barx1 expression is limited to the region surrounding the stomach, spleen and caudal surface of the liver, and does not extend into the mesenteric lining of intestinal loops (Fig. 6H,I and see Fig. S1 in the supplementary material). These data implicate mesothelial Barx1 expression in expansion and morphogenesis of adjacent spleen mesenchyme and segregation of the spleen from the dorsal pancreas.

Distinct pathways of Barx1 function in stomach and spleen development

Studies that combined Barx1 deficiency with a Wnt-reporter permitted us to ask whether Wnt signaling also occurs in the prospective spleen and if Barx1 might influence it. We did not detect β-gal activity at any point in the developing spleen in TOPGAL^{Tg} or

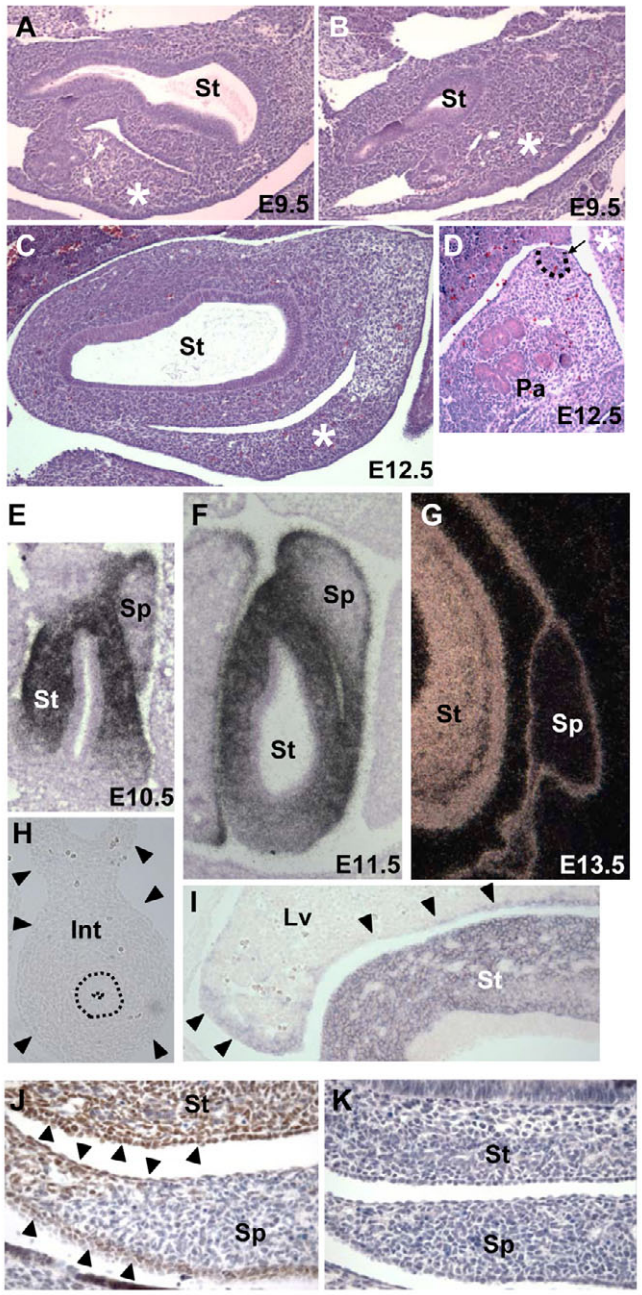

Fig. 6. Correlates of spleen development and Barx1 expression. (**A**,**B**) The spleen (*) appears to be specified correctly in E9.5 *Barx1*$^{-/-}$ mouse embryos (B), as in control littermates (A). St, stomach; Pa, pancreas. (**C**,**D**) Differences in size and organ relationships between control (C) and *Barx1*$^{-/-}$ (D) embryos are evident by E12.5 and increase thereafter. The position of the mutant spleen is again highlighted with a dotted line in D. (**E-G**) Radioactive mRNA in situ hybridization at E10.5, E11.5 and E13.5, showing high *Barx1* expression in stomach mesenchyme and mesothelium with exclusion from spleen mesenchyme throughout. Bright-field images are shown for the younger embryos and a dark-field image at E13.5. (**H**,**I**) Colorimetric mRNA in situ hybridization at E12.5, showing absence of *Barx1* expression in intestinal (Int; arrowheads in H) mesentery and presence in the mesothelial lining of the caudal liver (Lv; arrowheads in I), adjacent to the stomach (St). (**J**,**K**) Immunohistochemical confirmation with Barx1 (J) and preimmune (K) antiserum of high expression in stomach mesenchyme (top) and mesothelium (arrowheads), with exclusion from the spleen (Sp) mesenchyme in E12.5 embryos.

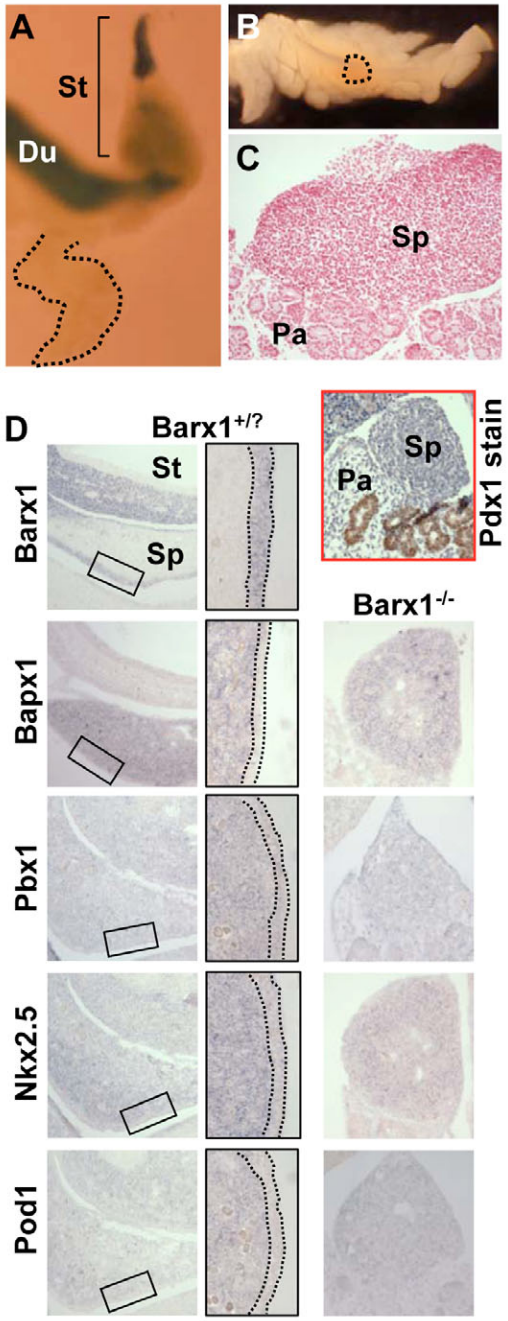

Fig. 7. Barx1 effects on the spleen are not mediated through either Wnt signaling or a group of homeodomain transcription factors implicated in control of spleen development. (**A-C**) Lack of β-gal activity in the pancreas or spleen of *Barx1*$^{-/-}$;TOPGAL E18.5 mouse embryos, shown in situ (A) to contrast with residual activity in the stomach (St) and native signal in duodenum (Du). The dotted line in A marks the fused spleen-pancreas (Pa), where absence of β-gal activity is further revealed in B and confirmed by microscopic analysis in C. (**D**) In contrast to *Barx1*, homeobox genes previously implicated in spleen development are mostly expressed in prospective spleen mesenchyme (Sp) and excluded from the mesothelium. The left column shows low-magnification images from each in situ hybridization, and the boxed area of each image is shown at higher magnification in the middle column, where the splenic capsule is demarcated by dotted lines. Images in the right-hand column reveal that expression of each of these homeobox genes is maintained in *Barx1*$^{-/-}$ spleen, which is recognized in part by juxtaposition to Pdx1^{+} pancreatic tissue (red box).

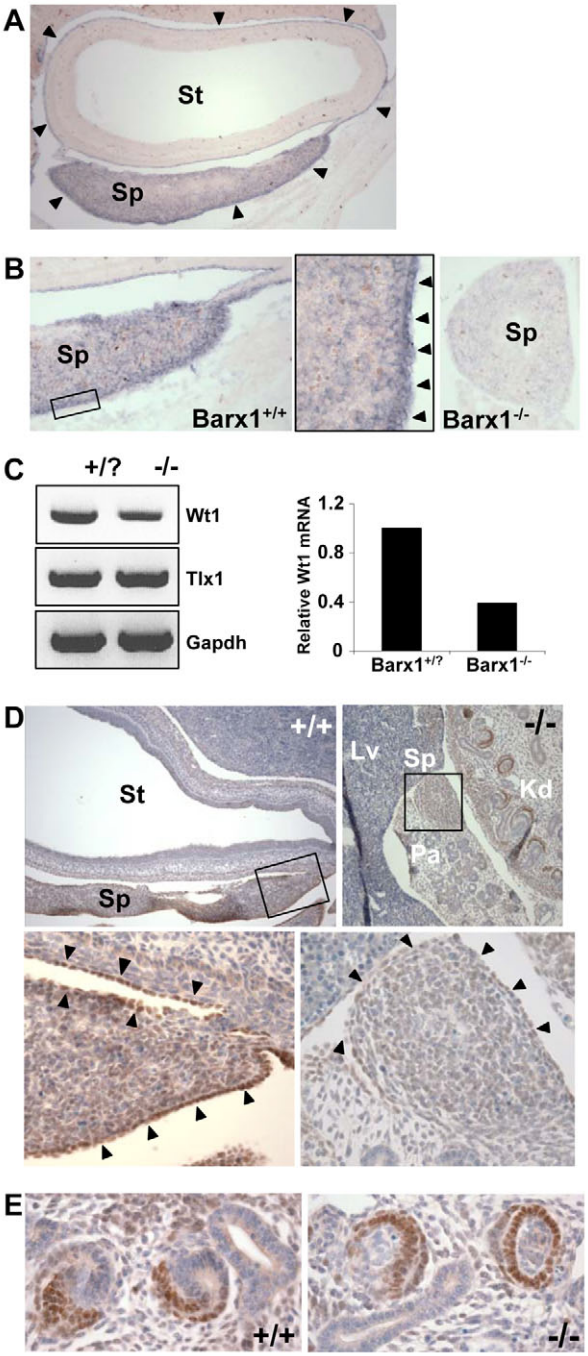

Fig. 8. Reduced expression of the multifunctional zinc-finger protein Wt1 in spleen mesothelium of *Barx1*$^{-/-}$ mice. (**A**) Among the genes previously implicated in spleen development, only expression of *Wt1* is readily recognized in the mesothelial lining (arrowheads) of wild-type E13.5 stomach (St) and spleen (Sp). (**B**) Higher magnification images of *Wt1* mRNA expression indicate enrichment in wild-type spleen capsule (the boxed area in the left panel is shown at even higher magnification in the middle panel, where arrowheads point to the outer surface) and substantially reduced levels in *Barx1*$^{-/-}$ spleen (right-hand panel). (**C**) Independent confirmation of reduced *Wt1* transcript levels, assessed by RT-PCR on RNA extracted from isolated E13.5 spleen and surrounding mesothelium. Products of conventional RT-PCR are shown in the gel on the left, and quantitation by real-time PCR using different primers in the bar chart on the right. For quantitative RT-PCR, values were first normalized for *Gapdh* expression and then to a value of 1.0 for control samples (+/? refers to +/+ or +/–). (**D**) Confirmation of reduced Wt1 expression by immunohistochemistry. Control (+/+) E13.5 stomach and spleen are shown in the left-hand panels and mutant tissues in the right-hand panels; the boxed areas in the upper panels are shown at higher magnification in the lower panels. Arrowheads point to the mesothelium, where Wt1 levels are reduced in *Barx1*$^{-/-}$ embryos. St, stomach; Sp, spleen; Pa, pancreas; Kd, kidney; Lv, liver. (**E**) Wt1 expression in *Barx1*$^{-/-}$ E13.5 kidney is intact.

Barx1$^{-/-}$;TOPGAL^{Tg} embryos (Fig. 7A-C and data not shown), which suggests that Barx1 controls spleen development through a different mechanism.

Mice carrying null mutations of the *Tlx1* (Dear et al., 1995; Roberts et al., 1994), *Bapx1* (*Nkx3-2* – Mouse Genome Informatics) (Lettice et al., 1999; Tribioli and Lufkin, 1999), *Pbx1* (Brendolan et al., 2005), *Wt1* (Herzer et al., 1999) or *Pod1* (*Tcf21* – Mouse Genome Informatics) (Lu et al., 2000) genes show splenic atrophy or asplenia, usually in conjunction with other defects. Mutant embryos typically initiate but fail to sustain spleen development as cells die, fail to proliferate, or change potential. *Bapx1*, *Pbx1* and *Tlx1* are early splenic markers and another homeobox gene, *Nkx2-5*, is also suspected to regulate spleen development (Brendolan et al., 2007). These factors therefore represent good candidates for dependence on Barx1 and their deficiencies might in part mediate aberrant spleen development in its absence. To address this possibility, we assessed expression in *Barx1*$^{-/-}$ mice of transcription factor genes implicated in spleen development. Expression of *Tlx1*, *Nkx2-5*, *Pbx1*, *Bapx1* and *Pod1* mRNAs appeared identical in *Barx1*$^{-/-}$ and control embryos (Fig. 7D) and β-gal staining in the splenic anlage of *Barx1*$^{-/-}$;*Tlx1*^{lacZ} embryos was indistinguishable from that in *Barx1*$^{+/-}$;*Tlx1*^{lacZ} littermates (data not shown).

Each of the transcripts we tested was expressed in the spleen primordium in wild-type mice, and incidentally also in stomach mesenchyme, but was absent from the mesothelial envelope (Fig. 7D). Only *Wt1* showed a distinctive pattern, with prominent mesothelial expression, similar or lower levels in splenic mesenchyme, and absence from stomach tissue (Fig. 8A). Thus, among the genes previously implicated in spleen development, *Wt1* is the best candidate for cell-autonomous regulation by mesothelial Barx1. Indeed, *Wt1* mRNA is appreciably reduced in *Barx1*$^{-/-}$ mesothelium (Fig. 8B), whereas *Barx1* mRNA expression is preserved in the embryonic stomach and mesothelium of *Wt1* mutants (B.-M.K., J. Alberta, D. Housman and R.A.S., unpublished). Conventional and quantitative RT-PCR confirmed reduced *Wt1* mRNA levels in isolated *Barx1*$^{-/-}$ spleen (Fig. 8C; residual expression is likely to derive from spleen mesenchyme), and Wt1 immunostaining in *Barx1*$^{-/-}$ and control embryos matched results from RNA in situ hybridization. We detected Wt1 in both wild-type and *Barx1*$^{-/-}$ spleen anlagen; signals were prominent in wild-type mesothelium and substantially reduced in *Barx1*-null spleen, particularly in the mesothelium (Fig. 8D). By contrast, Wt1 signals were preserved in embryonic kidney (Fig. 8E), the site of highest native expression.

DISCUSSION

Patterning of the vertebrate gastrointestinal tract serves as a model for fetal epithelial-mesenchymal interactions. In a quest for regulators of these interactions, we identified Barx1 as a factor that

is expressed abundantly, transiently and selectively in the mesenchyme and mesothelium of the developing stomach. We have now characterized its functions in development of the stomach and spleen and its powerful role as a homeotic regulator of abdominal organogenesis. Our results indicate that Barx1 influences development of two adjacent organs by different mechanisms: non-cell-autonomous inhibition of canonical Wnt signaling in stomach endoderm and cell-autonomous disruption of *Wt1* gene expression in splenic mesothelium.

Mice lacking Barx1 present a severe, invariant and completely penetrant form of visceral homeosis, with posteriorization of the proximal foregut. The esophagus is considerably shortened or, in the absence of markers that can distinguish mouse esophagus from squamous forestomach, might be missing entirely. Instead of the usual domed morphology, the fundic stomach is tubular, and cuboidal cells expressing neutral mucins and Muc5ac, which are usually confined to the glandular stomach, interrupt its squamous lining. Zones similarly blur in the body of the stomach, where cells normally restricted to the antrum/pylorus mix freely with corpus gland cells. By contrast, the next epithelial boundary is strictly preserved; intestinal villi occupy the entire distal stomach, but stomach and intestinal cells do not overlap in morphology or expression of regional markers. Homeosis in the *Barx1*$^{-/-}$ gut thus harbors unique features, with blurring of rostral organ and epithelial boundaries and anterior shifting of intestinal mucosa.

These gastrointestinal abnormalities extend away from the *Barx1* expression domain both rostrally (esophagus) and caudally (pyloric sphincter), a phenomenon that is reminiscent of homeotic transformations in the limbs and axial skeleton (Capecchi, 1996; Izpisua-Belmonte and Duboule, 1992). However, the major anomalies occur precisely in the domain of fetal Barx1 expression, in the gastric fundus and body, and suggest a dual role for Barx1 in stomach mesenchyme. One group of functions, likely to be intrinsic to the mesenchyme, drives sub-epithelial differentiation and generates the correct organ size and shape. Mesenchymal mass is reduced in *Barx1*$^{-/-}$ mice but its viability seems intact and smooth muscle appears in the right location; we have not addressed the mechanisms behind the role of Barx1 in stomach morphogenesis. A second group of non-cell-autonomous functions helps specify the overlying endoderm, as we previously inferred in part from findings in recombinant embryonic cell cultures (Kim et al., 2005). Our characterization of *Barx1*$^{-/-}$ stomach reinforces this function, extends our understanding and establishes the role of Barx1 in suppressing endodermal Wnt activity. We demonstrate that its absence permits persistent Wnt signaling in stomach endoderm, which is likely to disrupt mucosal specification and differentiation as a direct consequence. However, the scope of stomach and spleen defects in *Barx1*$^{-/-}$ embryos, coupled with the lack of canonical Wnt signaling in normal spleen primordium, implies that Wnt inhibition represents only a facet of Barx1 mechanisms, albeit one that is vital in stomach differentiation. Furthermore, we cannot rule out the possibility that Barx1 regulation of spleen morphogenesis also involves Wnt signaling through non-canonical pathways.

Unexpectedly, *Barx1*$^{-/-}$ mice have a misplaced and severely hypoplastic spleen of a form not observed in other animal models. Some reptiles (Falkmer, 1985) and mice lacking the pancreas-determining factor Ptf1a (Krapp et al., 1998) show isolated endocrine pancreatic progenitors scattered within the spleen. By contrast, *Barx1*$^{-/-}$ mice reveal a novel phenotype in which a discrete spleen is embedded within intact pancreatic parenchyma. Molecular understanding of spleen development is incomplete, but the organ is known to originate as a mesenchymal condensation within dorsal mesogastrium, in close apposition to the dorsal pancreas (Brendolan et al., 2007; Hecksher-Sorensen et al., 2004; Thiel and Downey, 1921). Mice with defects in late pancreas development, in which the mesenchyme is unaffected, usually have an intact spleen, whereas loss of pancreas mesenchyme, as observed, for example, in transgenic mice with ectopic Shh expression, is strongly correlated with asplenia (Ahlgren et al., 1996; Apelqvist et al., 1997; Harrison et al., 1999); these observations signify a role for dorsal pancreatic mesenchyme in some aspects of spleen development. However, *Barx1* mRNA and protein are conspicuously absent from spleen and pancreas anlagen, but appear at high levels in the epitheliod lining of these organ primordia. Barx1 is thus unique among regulators of spleen development in exerting a pivotal influence exclusively from the mesothelium and its expression pattern suggests that it moderates spleen development indirectly, much as mesenchymal Barx1 helps specify adjacent stomach endoderm. The splanchnic mesodermal plate is a known source of developmental signals, including fibroblast growth factors 9 and 10 (Hecksher-Sorensen et al., 2004). A key role for the prospective capsule in spleen development is independently revealed in dominant hemimelia (*Dh*) mutant mice, which lack this layer and are asplenic (Green, 1967; Hecksher-Sorensen et al., 2004); our findings suggest that some *Dh* effects might be mediated through Barx1.

All transcription factor genes expressed only in spleen primordium and previously implicated in its maturation are expressed normally in *Barx1*$^{-/-}$ spleen. These findings are consistent with the preservation of hematopoietic potential and indicate that Barx1 is dispensable for their expression. Features of the mutant phenotype point instead to functions not previously explored in spleen development. First, normal mesothelium seems to exert a Barx1-dependent trophic effect that enlarges the organ and imparts its characteristic shape. Alternatively, the mutant mesothelium might limit expansive and morphogenetic capacities inherent to the spleen anlage, and we cannot exclude the possibility that the spleen defects in *Barx1*$^{-/-}$ mice follow mainly from stomach malrotation and attendant disturbance in configuration of the omental bursa. A second function, separation of the spleen from the dorsal pancreas, is arguably better attributed to cell-autonomous properties of the mesothelium, and it is here that Wt1 loss might be especially pertinent. Unlike other genes implicated in the specification, survival or expansion of the spleen primordium, *Wt1* alone is expressed in the mesothelium (in addition to spleen mesenchyme); this overlap with the *Barx1* expression domain adds plausibility and significance to the result that mesothelial *Wt1* expression depends on Barx1. In both *Barx1*$^{-/-}$ and *Wt1*$^{-/-}$ embryos, the spleen is initially specified in the correct location and ultimately much reduced in size but not absent, and *Tlx1* expression is not perturbed. *Wt1*$^{-/-}$ spleen primordium is also reported to have a shorter connection to the prospective pancreas (Herzer et al., 1999), although perhaps not as short as we observe in *Barx1*$^{-/-}$ mice. Taken together, these observations raise the possibility that Barx1 control over spleen development might be exercised in part through *Wt1* gene regulation in the dorsal mesothelium. It is interesting that *Wt1* mRNA is reduced in *Tlx1*$^{-/-}$ splenic mesenchyme, but not in *Tlx1*$^{-/-}$ or *Pbx1*$^{-/-}$ mesothelium (Brendolan et al., 2005; Koehler et al., 2000).

Mice with targeted disruption of another homeobox gene, *Bapx1*, reveal markedly different consequences of failure of the spleen and dorsal pancreas to separate (Asayesh et al., 2006). *Bapx1*$^{-/-}$ pancreatic endoderm undergoes metaplastic conversion to intestinal cyst-like structures, a defect attributed to persistent contact with

spleen mesenchyme past E13.5, the stage by which the two organs have normally separated. The authors argued that other mouse models of asplenia avoid the same outcome because they do not expose the pancreatic epithelial primordium directly to spleen mesenchyme (Asayesh et al., 2006). As such contact is evident in *Barx1*$^{-/-}$ embryos, we suggest that either the metaplastic defect in *Bapx1*$^{-/-}$ pancreas is unique to that genotype, or the *Barx1*$^{-/-}$ spleen lacks the putative required factors.

Abdominal Barx1 expression is restricted to the stomach wall and mesothelium and we identify significant and distinct developmental functions in each of these locations. Our results also make a persuasive argument for Barx1-mediated inhibition of Wnt signaling in stomach endoderm and against a role for canonical Wnt signaling in spleen development. They hence demonstrate that positional and morphogenetic functions conferred by this homeobox gene occur through distinct mechanisms, even over the short distance that separates the stomach wall from its mesothelium. The pathways we have elucidated thus far – inhibition of canonical Wnt signaling in endoderm and regulation of *Wt1* gene expression in mesothelial cells – represent early steps in appreciating the basis for homeobox gene functions in the gastrointestinal tract. Barx1 is likely to regulate additional events that contribute not only to foregut patterning and spleen expansion, but also to control of stomach size and shape and pyloric sphincter formation. Characterization of other such pathways will add to the growing understanding of abdominal organogenesis.

This work was supported in part by grant number R01DK61139 (R.A.S.) and R01NS033642 (A.P.M.) from the National Institutes of Health. J.M. is a fellow of the Charles H. Hood Foundation. We are grateful to Susumu Ito for assistance with electron microscopy; Zhao Chen and SunTaek Kim for help with flow cytometry; Walter Birchmeier for providing *Axin2*^{lacZ} reporter mice; Cliff Tabin and Mark Taketo for sharing *Shh*^{Cre} and *Catnb*$^{lox(ex3)}$ mice, respectively; Terry Rabbitts and Licia Selleri for providing *Tlx1*^{lacZ} mice; Julia Alberta and David Housman for sharing *Wt1*-mutant mouse embryos; Christopher Wright and David Alper for generous gifts of Pdx1 and intrinsic factor antisera, respectively; Richard Harvey, Thomas Lufkin, Robert Schwartz and Licia Selleri for plasmids; and Andrea Brendolan, Licia Selleri and Mike Verzi for critical review of the manuscript.

Supplementary material

Supplementary material for this article is available at http://dev.biologists.org/cgi/content/full/134/20/3603/DC1

References

Ahlgren, U., Jonsson, J. and Edlund, H. (1996). The morphogenesis of the pancreatic mesenchyme is uncoupled from that of the pancreatic epithelium in IPF1/PDX1-deficient mice. *Development* **122**, 1409-1416.

Apelqvist, A., Ahlgren, U. and Edlund, H. (1997). Sonic hedgehog directs specialized mesoderm differentiation in the intestine and pancreas. *Curr. Biol.* **7**, 801-804.

Asayesh, A., Sharpe, J., Watson, R. P., Hecksher-Sorensen, J., Hastie, N. D., Hill, R. E. and Ahlgren, U. (2006). Spleen versus pancreas: strict control of organ interrelationship revealed by analyses of Bapx1–/– mice. *Genes Dev.* **20**, 2208-2213.

Brendolan, A., Ferretti, E., Salsi, V., Moses, K., Quaggin, S., Blasi, F., Cleary, M. L. and Selleri, L. (2005). A Pbx1-dependent genetic and transcriptional network regulates spleen ontogeny. *Development* **132**, 3113-3126.

Brendolan, A., Rosado, M. M., Carsetti, R., Selleri, L. and Dear, T. N. (2007). Development and function of the mammalian spleen. *BioEssays* **29**, 166-177.

Capecchi, M. R. (1996). Function of homeobox genes in skeletal development. *Ann. N. Y. Acad. Sci.* **785**, 34-37.

Chinery, R., Poulsom, R., Rogers, L. A., Jeffery, R. E., Longcroft, J. M., Hanby, A. M. and Wright, N. A. (1992). Localization of intestinal trefoil-factor mRNA in rat stomach and intestine by hybridization in situ. *Biochem. J.* **285**, 5-8.

Clevers, H. (2006). Wnt/beta-catenin signaling in development and disease. *Cell* **127**, 469-480.

DasGupta, R. and Fuchs, E. (1999). Multiple roles for activated LEF/TCF transcription complexes during hair follicle development and differentiation. *Development* **126**, 4557-4568.

Dear, T. N., Colledge, W. H., Carlton, M. B., Lavenir, I., Larson, T., Smith, A. J., Warren, A. J., Evans, M. J., Sofroniew, M. V. and Rabbitts, T. H. (1995). The Hox11 gene is essential for cell survival during spleen development. *Development* **121**, 2909-2915.

Echelard, Y., Epstein, D. J., St-Jacques, B., Shen, L., Mohler, J., McMahon, J. A. and McMahon, A. P. (1993). Sonic hedgehog, a member of a family of putative signaling molecules, is implicated in the regulation of CNS polarity. *Cell* **75**, 1417-1430.

Falkmer, S. (1985). Comparative morphology of pancreatic islets in animals. In *The Diabetic Pancreas* (ed. B. W. Volk and K. F. Wellmann), pp. 17-52. New York: Plenum Press.

Finch, P. W., He, X., Kelley, M. J., Uren, A., Schaudies, R. P., Popescu, N. C., Rudikoff, S., Aaronson, S. A., Varmus, H. E. and Rubin, J. S. (1997). Purification and molecular cloning of a secreted, Frizzled-related antagonist of Wnt action. *Proc. Natl. Acad. Sci. USA* **94**, 6770-6775.

Green, M. C. (1967). A defect of the splanchnic mesoderm caused by the mutant gene dominant hemimelia in the mouse. *Dev. Biol.* **15**, 62-89.

Harada, N., Tamai, Y., Ishikawa, T., Sauer, B., Takaku, K., Oshima, M. and Taketo, M. M. (1999). Intestinal polyposis in mice with a dominant stable mutation of the beta-catenin gene. *EMBO J.* **18**, 5931-5942.

Harfe, B. D., Scherz, P. J., Nissim, S., Tian, H., McMahon, A. P. and Tabin, C. J. (2004). Evidence for an expansion-based temporal Shh gradient in specifying vertebrate digit identities. *Cell* **118**, 517-528.

Harrison, K. A., Thaler, J., Pfaff, S. L., Gu, H. and Kehrl, J. H. (1999). Pancreas dorsal lobe agenesis and abnormal islets of Langerhans in Hlxb9-deficient mice. *Nat. Genet.* **23**, 71-75.

Hecksher-Sorensen, J., Watson, R. P., Lettice, L. A., Serup, P., Eley, L., De Angelis, C., Ahlgren, U. and Hill, R. E. (2004). The splanchnic mesodermal plate directs spleen and pancreatic laterality, and is regulated by Bapx1/Nkx3.2. *Development* **131**, 4665-4675.

Herzer, U., Crocoll, A., Barton, D., Howells, N. and Englert, C. (1999). The Wilms tumor suppressor gene wt1 is required for development of the spleen. *Curr. Biol.* **9**, 837-840.

Izpisua-Belmonte, J. C. and Duboule, D. (1992). Homeobox genes and pattern formation in the vertebrate limb. *Dev. Biol.* **152**, 26-36.

Jho, E. H., Zhang, T., Domon, C., Joo, C. K., Freund, J. N. and Costantini, F. (2002). Wnt/beta-catenin/Tcf signaling induces the transcription of Axin2, a negative regulator of the signaling pathway. *Mol. Cell. Biol.* **22**, 1172-1183.

Kanzler, B. and Dear, T. N. (2001). Hox11 acts cell autonomously in spleen development and its absence results in altered cell fate of mesenchymal spleen precursors. *Dev. Biol.* **234**, 231-243.

Karam, S. M. and Leblond, C. P. (1992). Identifying and counting epithelial cell types in the "corpus" of the mouse stomach. *Anat. Rec.* **232**, 231-246.

Kim, B. M., Buchner, G., Miletich, I., Sharpe, P. T. and Shivdasani, R. A. (2005). The stomach mesenchymal transcription factor Barx1 specifies gastric epithelial identity through inhibition of transient Wnt signaling. *Dev. Cell* **8**, 611-622.

Koehler, K., Franz, T. and Dear, T. N. (2000). Hox11 is required to maintain normal Wt1 mRNA levels in the developing spleen. *Dev. Dyn.* **218**, 201-216.

Krapp, A., Knofler, M., Ledermann, B., Burki, K., Berney, C., Zoerkler, N., Hagenbuchle, O. and Wellauer, P. K. (1998). The bHLH protein PTF1-p48 is essential for the formation of the exocrine and the correct spatial organization of the endocrine pancreas. *Genes Dev.* **12**, 3752-3763.

Lettice, L. A., Purdie, L. A., Carlson, G. J., Kilanowski, F., Dorin, J. and Hill, R. E. (1999). The mouse bagpipe gene controls development of axial skeleton, skull, and spleen. *Proc. Natl. Acad. Sci. USA* **96**, 9695-9700.

Lu, J., Chang, P., Richardson, J. A., Gan, L., Weiler, H. and Olson, E. N. (2000). The basic helix-loop-helix transcription factor capsulin controls spleen organogenesis. *Proc. Natl. Acad. Sci. USA* **97**, 9525-9530.

Offield, M. F., Jetton, T. L., Labosky, P. A., Ray, M., Stein, R. W., Magnuson, M. A., Hogan, B. L. and Wright, C. V. (1996). PDX-1 is required for pancreatic outgrowth and differentiation of the rostral duodenum. *Development* **122**, 983-995.

Que, J., Okubo, T., Goldenring, J. R., Nam, K. T., Kurotani, R., Morrisey, E. E., Taranova, O., Pevny, L. H. and Hogan, B. L. (2007). Multiple dose-dependent roles for Sox2 in the patterning and differentiation of anterior foregut endoderm. *Development* **134**, 2521-2531.

Rattner, A., Hsieh, J. C., Smallwood, P. M., Gilbert, D. J., Copeland, N. G., Jenkins, N. A. and Nathans, J. (1997). A family of secreted proteins contains homology to the cysteine-rich ligand-binding domain of frizzled receptors. *Proc. Natl. Acad. Sci. USA* **94**, 2859-2863.

Roberts, C. W., Shutter, J. R. and Korsmeyer, S. J. (1994). Hox11 controls the genesis of the spleen. *Nature* **368**, 747-749.

Silberg, D. G., Swain, G. P., Suh, E. R. and Traber, P. G. (2000). Cdx1 and cdx2 expression during intestinal development. *Gastroenterology* **119**, 961-971.

Soriano, P. (1999). Generalized lacZ expression with the ROSA26 Cre reporter strain. *Nat. Genet.* **21**, 70-71.

Thiel, G. A. and Downey, H. (1921). The development of the mammalian spleen with special reference to its hematopoietic activity. *Am. J. Anat.* **28**, 279-339.

Tissier-Seta, J. P., Mucchielli, M. L., Mark, M., Mattei, M. G., Goridis, C. and Brunet, J. F. (1995). Barx1, a new mouse homeodomain transcription factor expressed in cranio-facial ectomesenchyme and the stomach. *Mech. Dev.* **51**, 3-15.

Tribioli, C. and Lufkin, T. (1999). The murine Bapx1 homeobox gene plays a critical role in embryonic development of the axial skeleton and spleen. *Development* **126**, 5699-5711.

Yu, H. M., Jerchow, B., Sheu, T. J., Liu, B., Costantini, F., Puzas, J. E., Birchmeier, W. and Hsu, W. (2005). The role of Axin2 in calvarial morphogenesis and craniosynostosis. *Development* **132**, 1995-2005.